

Selective Area Growth by Metal Organic Vapor Phase Epitaxy and Atomic Layer Epitaxy Using Ga₂O₃ as a Novel Mask Layer

Shingo HIROSE*, Akihiro YOSHIDA¹, Masaaki YAMAURA¹, Kazuhiko HARA¹ and Hiro MUNEKATA¹

Mechanical Engineering Laboratory, AIST, MITI, 1-2 Namiki, Tsukuba, Ibaraki 305-8564, Japan

¹*Imaging Science and Engineering Laboratory, Tokyo Institute of Technology, 4259 Nagatsuda, Midori-ku, Yokohama 226-8503, Japan*

(Received September 1, 1998; accepted for publication January 7, 1999)

A novel technique is proposed for advanced microstructure formation using Ga₂O₃ as a new mask material. Ga₂O₃ layers were prepared by RF sputtering with Ga₂O₃ powder target and patterned using photolithography. Scanning electron microscope (SEM) and Photoluminescence (PL) measurement findings indicate that reasonably high-quality single crystalline GaAs layers could be successfully grown selectively on the unmasked region by metal organic vapor phase epitaxy (MOVPE) and atomic layer epitaxy (ALE). The GaAs/AlGaAs quantum structure was also fabricated by selective area MOVPE, however, at this stage, polycrystalline AlGaAs layers formed on the mask region after the mask removal and the regrowth of AlGaAs overlayers. The key factor in this microstructure fabrication process is the sensitive dependence of Ga oxide layers against the reactor pressure under H₂ exposure.

KEYWORDS: selective area growth, Ga₂O₃, metal organic vapor phase epitaxy, atomic layer epitaxy, GaAs, AlGaAs

1. Introduction

Selective area growth (SAG) has been widely studied for various microstructure fabrications. Many different mask materials such as SiO₂,^{1,2} SiN_x,^{3,4} Al₂O₃,⁵ In₂O₃,⁶ AlN,⁷ have been used for SAG of III–V compounds. Since, to form the buried structure using these mask materials, the mask layer must be removed by chemical etching at outside the chamber, surface contamination and damage are difficult to prevent. This may be a serious problem when decreasing the scale of the microstructure because impurities and defects from etching degrade electrical and optical properties due to the formation of an inactivated center.

On the other hand, Ga₂O₃ is very suitable for SAG for three main reasons: (1) As the most chemically stable of the Ga- and As-related oxides, it can survive during growth,⁸ (2) it can be eliminated immediately in the growth reactor by thermal treatment with H₂ exposure,⁹ and (3) the interface quality between the GaAs and Ga₂O₃ layers is very high.¹⁰ We have inferred that these qualities may be applicable to advanced microstructure fabrications.

Figure 1 illustrates an example of the microstructure fabrication process we proposed in this study. Firstly, Ga₂O₃ layers are deposited by RF sputtering on the GaAs substrate. Then, portions of the Ga₂O₃ layers are removed using lithographic techniques. Next, GaAs and AlGaAs layers are grown selectively on unmasked areas. After SAG, the Ga₂O₃ mask layers are removed in the same reactor by thermal treatment. Finally, AlGaAs regrowth is used to bury the entire fine structure. This fabrication process has two advantages: one is that the surface deterioration, which is caused by exposure to the atmosphere, is negligible. The other is that the use of the Ga₂O₃ mask simplifies the fabrication process because it does not need to be removed at outside the chamber.

In order to experimentally prove our microstructure fabrication process using Ga₂O₃ as a novel mask material, we have investigated a fabrication process which consists of mask formation, patterning, SAG by metal organic vapor phase epitaxy (MOVPE) and atomic layer epitaxy (ALE), mask removal, and regrowth. A similar method of using a Ga₂O₃

mask has been already demonstrated with the molecular beam epitaxy (MBE) growth system.¹¹

However, no successful growth of a hetero-microstructure has been reported. We should also mention that, as far as we know, no one has reported on a SAG process using MOVPE as we have, although SAG using GaAs oxidation as the mask has been already confirmed.¹² MOVPE is more suitable than MBE in principle because of its mass-production capability and the use of the volatile arsenic element, therefore we employed the MOVPE technique for growth. Moreover, compared to MOVPE and MBE, ALE offers greater thickness uniformity and less anonymous edge growth in selective epitaxy. Therefore, we also adopted ALE growth in this study.

2. Experimental Details

Ga₂O₃ films were deposited by RF sputtering under the following conditions. The Ga₂O₃ target was a powder source with a purity of 5 N (99.999%). Argon and oxygen were used with supply rates of 3.7×10^{-1} – $1.5 \mu\text{mol/s}$ and 3.7×10^{-1} – $7.4 \mu\text{mol/s}$, respectively. RF plasma power was changed between 50 and 300 W. The reactor pressure (P_r) and the substrate temperature (T_s) were kept constant during sputtering, typically at 6×10^{-3} Torr and at 100°C, respectively. These conditions result in a deposition rate of 10 to 40 nm per hour.

The growth system was conventional low pressure MOVPE. Trimethylgallium [(CH₃)₃Ga; TMGa], ethyldimethylamine alane [C₂H₅(CH₃)₂N:AlH₃; EDMAAl] and a 20% mixture of arsine [AsH₃] in hydrogen were used as the gallium, aluminum and arsenic sources, respectively. TMGa and AsH₃ flow rates were 3.7×10^{-2} – $1.5 \times 10^{-1} \mu\text{mol/s}$ and 1.5 – $3.0 \times 10^1 \mu\text{mol/s}$, respectively. We used LEC semi-insulating GaAs substrates having a (001) orientation.

The surface morphologies and crosssection profiles were inspected using a surface profiler (DEKTAK 3) and field emission scanning electron microscope (FE-SEM). Photoluminescence (PL) measurements were made under the excitation of a helium-cadmium laser at 442 nm to check the crystallinity of the grown layers. Carbon concentration was measured using a CAMECA IMS 4f secondary ion mass spectrometry (SIMS) with Cs⁺ primary beam in the negative

*E-mail: hirose@mel.go.jp

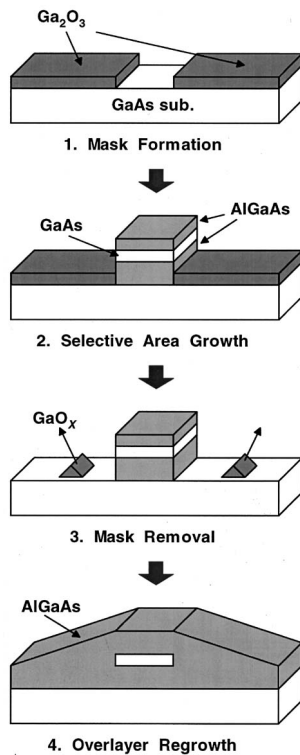


Fig. 1. Scheme for proposed in-situ SAG using Ga_2O_3 mask: (1) formation of mask layer; (2) SAG by MOVPE; (3) mask removal of mask layer and (4) re-growth by MOVPE.

secondary ion-detection mode.

3. Formation and Quality of Mask Layer

Figure 2 shows scanning electron microscope (SEM) images of the Ga_2O_3 surface. When the RF power and oxygen gas supply rate were fixed at 300 W and $1.5 \mu\text{mol/s}$, respectively, many pinholes were observed on the oxide surface. When the RF power was decreased to 50 W while increasing the O_2 gas supply to $7.4 \mu\text{mol/s}$, the surface of the oxide films became flat and the morphology was drastically improved, as seen in Fig. 2(b). Sputtering conditions were optimized in this way.

Next, we investigated the quality of the mask layer. Absorption measurements were taken on 240 nm thick Ga_2O_3 layers deposited on the glass substrate. The fundamental absorption edge of the Ga_2O_3 layers was estimated to be 4.4 eV, which was very close to the 4.8 eV reported.^{13,14} Furthermore, no X-ray diffraction peak was observed from the oxide layers, and reflection high energy electron diffraction (RHEED) measurements also showed a halo pattern for the oxide layers. These results indicated that amorphous oxide layers were obtained by the RF sputtering.

4. Patterning of Mask Layer

Ga_2O_3 mask layers can be etched by BHF, but cannot be removed by H_2SO_4 solution. We took advantage of this characteristic by patterning the substrate using the following process. First, the Ga_2O_3 mask layers were deposited on the GaAs substrate. Next, Ga_2O_3 layers were resist coated. The Ga_2O_3 layers were etched using BHF solution at a rate of 90 to 120 nm/min. Then, an acid solution, consisting of $1 \text{H}_2\text{SO}_4 : 1 \text{H}_2\text{O}_2 : 100 \text{H}_2\text{O}$, was used to etch the GaAs lay-

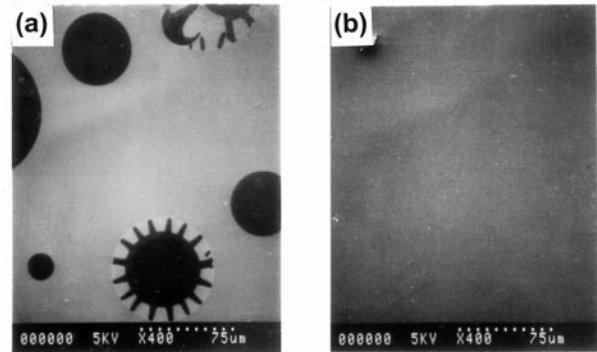


Fig. 2. SEM images of Ga_2O_3 surface after RF sputtering. Reactor pressure was 46×10^{-4} Torr, at substrate temperature of 100°C . Plasma conditions were (a) 300 W RF power, O_2 at $1.5 \mu\text{mol/s}$; (b) 50 W RF power, O_2 at $7.4 \mu\text{mol/s}$.

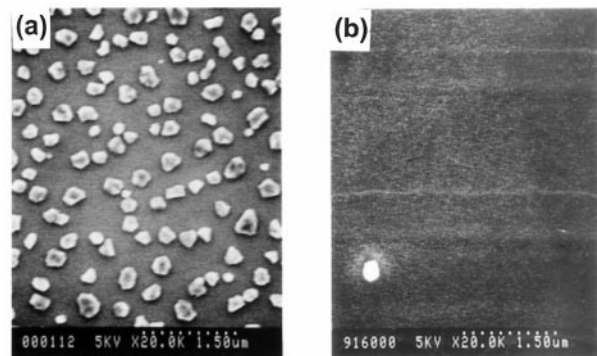


Fig. 3. SEM images of Ga_2O_3 surface after H_2 and AsH_3 exposure. Reactor pressure was (a) 100 Torr and (b) 10 Torr when H_2 and AsH_3 were 5 slm and $3.0 \times 10^1 \mu\text{mol/s}$, respectively.

ers slightly. Stripes were parallel to the [10] direction. Since a positive resist was more easily removed after patterning than a negative resist, the positive resist was selected for the resist layers. Patterning was successfully achieved to a mask layer height of 10 nm.

5. Stability of Mask Layer

Next, we investigated the stability of the mask layer. Figure 3 shows SEM images of the Ga_2O_3 surface after H_2 and AsH_3 exposure. H_2 and AsH_3 were fixed at 5 slm and $3.0 \times 10^1 \mu\text{mol/s}$, respectively. At the reactor pressure (P_r) of 100 Torr with H_2 and AsH_3 exposure, the Ga_2O_3 layers deoxidized at over $T_s = 480^\circ\text{C}$, and turned to GaAs islands on the mask surface by reacting with AsH_3 [Fig. 3(a)]. In contrast, by changing the reactor pressure from 100 Torr to 10 Torr, oxide layers were not sublimated even, when we increased T_s up to 750°C [Fig. 3(b)]. The decrease in the reactor pressure corresponds to an increase in hydrogen flow speed when the hydrogen supply rate is fixed. It is clear that the hydrogen flow speed at the reactor pressure of 10 Torr is one order of magnitude faster than that at $P_r = 100$ Torr. Furthermore, the increase in the hydrogen flow speed also suggests that the timing of the hydrogen attack on the mask surface was shortened. We can tentatively conclude that it was so short that mask desorption hardly occurred at $P_r = 10$ Torr. On the basis of these findings, we can assume that SAG should be done under a reactor pressure of 10 Torr, and the mask removal process must

be done at more than 100 Torr.

6. Selective Area Growth

Both MOVPE and ALE were utilized for selective area growth. Figure 4 shows SEM images of crosssections of MOVPE-grown samples with different V/III ratio. At V/III ratio = 800 with $T_s = 640^\circ\text{C}$, GaAs layers were deposited on both the masked and unmasked areas [Fig. 4(a)]. On the other hand, by reducing the V/III ratio = 20, and increasing T_s to 720°C , epitaxial growth occurred only on the unmasked area, resulting in a perfect SAG [Fig. 4(b)]. SIMS analysis showed no undesirable deposition on the mask region within the measurement limits of 4 nm. The sensitive dependence of growth selectivity on the growth conditions can probably be explained in terms of the As- and T_s -dependence of the migration rate of Ga species. Under lower V/III ratio growth conditions, it is probable that gallium species freely diffuse on the mask surface because of the weakness of the chemical reaction between the Ga species and the mask films. On the other hand, at a higher V/III ratio, the adsorbed Ga species remain on the mask surface, causing the growth of GaAs to occur by reacting with AsH_3 . In addition, the increase in the operating temperature (T_s) may be expected to give us longer diffusion length so that the migration on the mask would be enhanced. In this study, the increase in the operating temperature (T_s) was somewhat less a factor in obtaining the growth selectivity than the change of the V/III ratio of the reactant species.

Figure 5 shows PL spectra at 20 K of selective area MOVPE-grown GaAs with different stripe widths of (a) 1.0 mm and (b) $10\ \mu\text{m}$, respectively. The PL spectrum from the 1.0 mm wide stripes consisted of near band-edge emission of 1.51 eV and carbon related emission of 1.49 eV [Fig. 5(a)]. This PL behavior showed that the quality of our obtained epitaxial GaAs layers was the same as the reported high-quality undoped GaAs layers.¹⁵⁾ On the other hand, by decreasing the GaAs stripe width from 1.0 mm to $10\ \mu\text{m}$, the PL spectrum was dominated by donor-acceptor pair emission located at 1.48 eV [Fig. 5(b)]. It is likely that the decrease of the GaAs stripe width increases carbon incorporation in the GaAs layers. The actual V/III ratio might be different at the edge and the center of the GaAs stripes, and this is a problem to be overcome for SAG at decreased structure scales.

Next, we tried to grow AlGaAs on a patterned substrate

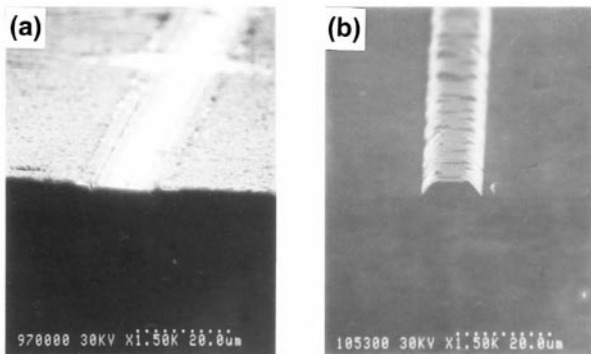


Fig. 4. SEM photographs of patterned surface after MOVPE growth of GaAs. Stripe width of unmasked region was $10\ \mu\text{m}$. Growth conditions: (a) V/III ratio = 800 at $T_s = 640^\circ\text{C}$ and (b) V/III ratio = 20 at $T_s = 720^\circ\text{C}$.

with a stripe width of $25\ \mu\text{m}$. Figure 6 shows SEM images of AlGaAs layer crosssections of grown by MOVPE. Ethyldimethylamine alane (EDMAAl) and trimethylgallium (TMGa) supply rates were $7.4 \times 10^{-3}\ \mu\text{mol/s}$ and $7.4 \times 10^{-2}\ \mu\text{mol/s}$, respectively. We first grew the AlGaAs layers under growth conditions in which high-quality AlGaAs layers could be grown on an unmasked substrate. While maintaining AsH_3 supply at $3.0 \times 10^{-1}\ \mu\text{mol/s}$ and $T_s = 720^\circ\text{C}$, as clearly seen in Fig. 6(a), single crystalline AlGaAs layers were epitaxially grown on the GaAs surface. However, AlGaAs polycrystalline layers overlapped at the mask regions. In the case of SAG of GaAs, it was found that a low V/III ratio and a high T_s , which enhanced the surface migration rate, are particularly important for achieving the growth selectivity. So, we decreased the AsH_3 supply rate to $1.5 \times 10^{-1}\ \mu\text{mol/s}$ while keeping T_s at 730°C . After SAG under these growth conditions, the AlGaAs layers were successfully grown on only the unmasked regions, while the other areas were not covered, although there were tiny holes on the surface [Fig. 6(b)]. Further investigation is needed to optimize the growth conditions.

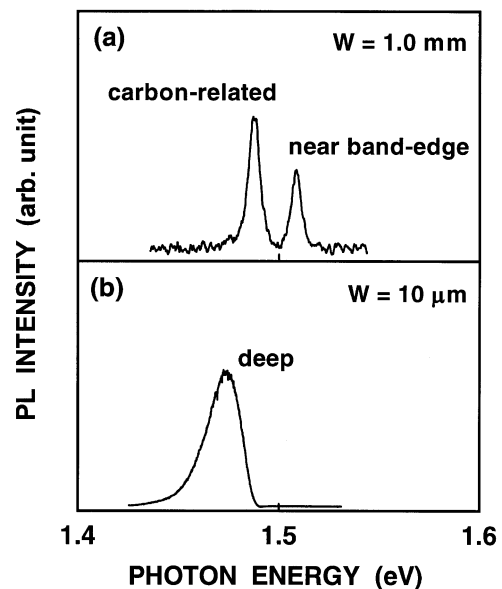


Fig. 5. PL spectra of selectively grown GaAs layers at unmasked region. Stripe widths of unmasked region were (a) 1.0 mm and (b) $10\ \mu\text{m}$.

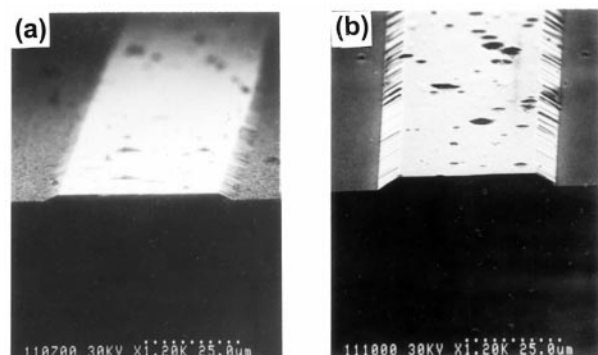


Fig. 6. SEM photographs of patterned surface after MOVPE growth of AlGaAs layers. Stripe width of unmasked region was $30\ \mu\text{m}$. AsH_3 supply rates were (a) $3.0 \times 10^{-1}\ \mu\text{mol/s}$ and (b) $1.5 \times 10^{-1}\ \mu\text{mol/s}$.

By combining SAG of GaAs with AlGaAs, we attempted to fabricate single quantum well structures. Figure 7 shows the PL spectra of GaAs quantum wells grown selectively on 50 μm wide stripes. The thickness of the GaAs well and AlGaAs barrier layers were 10 nm and 3 μm , respectively. The excitation energy was fixed at 2.8 eV. The PL peak located at 1.89 eV is dominated by the emission from the AlGaAs layers. It can be estimated from this peak position that the Al composition ratio in the AlGaAs layers is about 35.8% as we speculated from the growth conditions. Another sharp peak located at 1.49 eV and an additional broad peak at around 1.55 eV were attributed to the GaAs layers. The sharp peak corresponds to the carbon related emission peak that is observed in PL emission spectrum from GaAs layers. The additional broad peak at around 1.55 eV would originate from the emission of the GaAs-related layers. Assuming that a single GaAs-well-layer was sandwiched between $\text{Al}_x\text{Ga}_{1-x}\text{As}$ barrier layers, the position of the PL emission from single quantum well structures would be expected to appear at 1.55 eV from the numerical calculation curve for $x = 0.36$.¹⁶⁾ This value is very consistent with any measurement at 1.55 eV. We can thus assume that single quantum well structures can be successfully fabricated by the SAG method. However, since the PL peak is rather broad, which is probably due to the fluctuation of the GaAs wells, further improvement in quality of the GaAs/AlGaAs well structures is required.

Similarly, we investigated selective area ALE using a Ga_2O_3 mask. Figure 8 shows the crosssection profile of samples (a) before and (b) after ALE growth. As seen in Fig. 8(a), the height of the Ga_2O_3 mask layers on the substrate was estimated to be 40 nm, which was larger than that of the GaAs on the unmasked region. We then applied ALE to this sample. The growth conditions, in which the growth rate was controlled by the number of source supply cycles, were as follows. TMGa and AsH_3 were supplied at $3.7 \times 10^{-1} \mu\text{mol/s}$ and $3.0 \times 10^1 \mu\text{mol/s}$, respectively. The source supply cycle consisted of 3 s H_2 purge, 10 s TMGa, 3 s H_2 purge and 10 s AsH_3 . After ALE growth, a 50 nm high GaAs layer was established on only the GaAs region, and what is more, overlay GaAs growth on the mask region was completely pre-

vented [Fig. 8(b)]. Neither anonymous edge growth nor facet development was seen in ALE. Even at a wide GaAs stripe of 1.0 mm, growth selectivity between GaAs and Ga_2O_3 was clearly achieved.⁹⁾

Figure 9 shows PL spectra at 20 K of ALE-grown GaAs layers on a patterned substrate. The PL spectrum was dominated only by acceptor-related emission. The FWHM of the PL emission peak was 15 meV. SIMS measurement also showed that the amount of carbon incorporation in GaAs obtained by selective area ALE was $2.0 \times 10^{18} \text{cm}^{-3}$. It should be mentioned that these PL characteristics and the carbon content were almost the same as for ALE-grown GaAs layers on non-patterned substrate, and can thus be considered

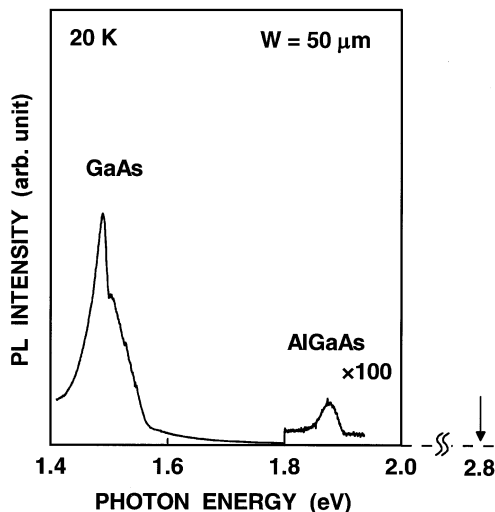


Fig. 7. PL spectra of GaAs/AlGaAs quantum well structures. The thicknesses of barrier and well layers were 2 nm and 10 nm, respectively.

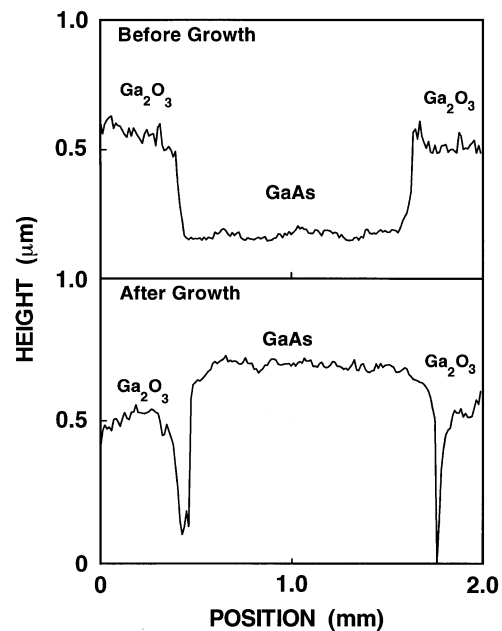


Fig. 8. Crosssection profiles for patterned substrate (a) before and (b) after ALE growth of GaAs. Stripe width of unmasked region was 1.0 mm.

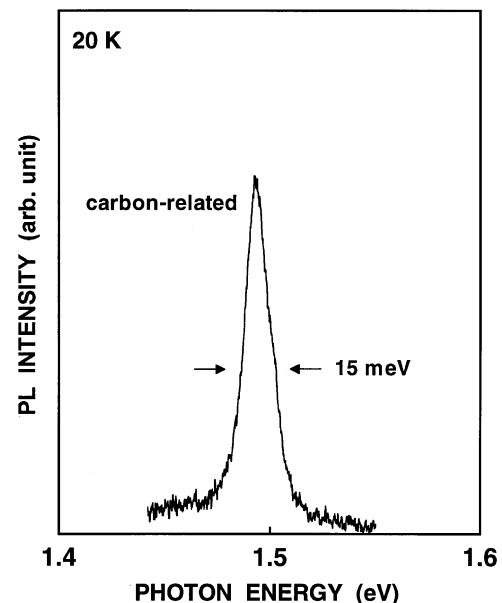


Fig. 9. PL spectra at 20 K of ALE-grown GaAs layers on unmasked areas. Stripe width of unmasked region was 1.0 mm.

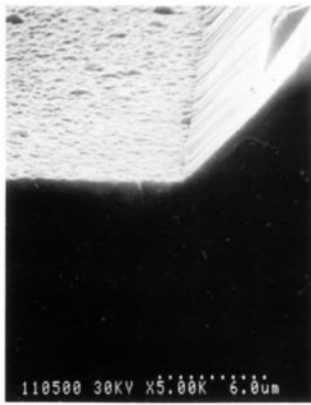


Fig. 10. Crosssection SEM image of the AlGaAs/GaAs/AlGaAs buried structure after overlayer MOVPE regrowth of AlGaAs.

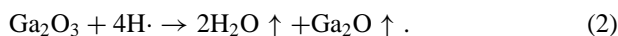
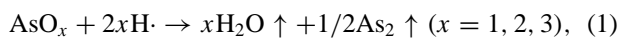
independent of the existence of the mask layer. Therefore, the crystal quality of the GaAs layers grown by selective area ALE can be considered reasonably good.

7. Mask Removal and Regrowth

GaAs/AlGaAs double heterostructures, grown by selective area MOVPE on patterned substrate, were used to investigate mask removal and AlGaAs overlayer regrowth process. Thermal treatment by H_2 at $T_s = 640^\circ C$ and $P_r = 500$ Torr was employed to remove the oxide mask layers. To ensure stability whether the mask layers were removed perfectly or not, we grew AlGaAs overlayers to bury the entire GaAs/AlGaAs double heterostructures. Because the mask layers were so thin their existence could not be quantitatively identified.

Unexpectedly, however, polycrystalline AlGaAs islands deposited on the mask layers after the MOVPE regrowth of the AlGaAs overlayers, while single crystalline AlGaAs layers were epitaxially grown on the surface fabricated heterostructures (Fig. 10). Considering the fact that single crystalline AlGaAs layers were always grown completely even on extremely rough surfaces under these growth conditions for the AlGaAs overlayers, it can be assumed that the mask layers were only partially removed by H_2 annealing on the oxide surface, and therefore polycrystalline AlGaAs layers were formed during the AlGaAs overlayer regrowth.

It was considered that GaAs oxide could be removed from the surface through the next reaction passway;⁸⁾



So, in order to enable the removal of the mask, hydrogen radical irradiation was adopted to remove residual mask layers as an additional reaction process. After SAG of AlGaAs/GaAs/AlGaAs structures on the patterned substrate, the sample was loaded to another oxide chamber and was exposed in mild

hydrogen-plasma (40 W, $T_s = 480^\circ C$, 180 min), and then it was inserted into the MOVPE reactor again. Although the removal of the mask layer was slightly enhanced by the above-mentioned process, many polycrystals still deposited on the mask region. And this remains a problem yet to be solved.

8. Conclusions

We have proposed and demonstrated a novel microstructure fabrication process of SAG using MOVPE and ALE of Ga_2O_3 as a new mask. We have found that Ga_2O_3 mask layers formed by RF sputtering could be patterned by photolithography. The oxide layers were stable at a low reactor pressure of 10 Torr, but eliminated by H_2 exposure at a relatively high reactor pressure. Reasonably good single crystalline GaAs layers and GaAs/AlGaAs quantum well structures were fabricated selectively on the unmasked region by using this new mask. However, mask removal and regrowth processes after SAG were not satisfactory for our requirement at this stage: many polycrystals were observed on the mask region because the removal of the mask was incomplete, although hydrogen radical irradiation proved to be effective in the mask removal process.

Acknowledgements

The authors are deeply grateful to Emeritus Professor H. Kukimoto for his continuing encouragement. We would like to express our special thanks to Dr. K. Watanabe and Mr. M. Momose for their valued contributions and kind cooperation. We also wish to express our appreciation to Taiyo-Toyo Sanso Co., Ltd. for supplying arsine gas. This study was supported in part by Research Fellowships of the Japan Society for the Promotion of Science for Young Scientists.

- 1) C. Ghosh and R. L. Layman: Appl. Phys. Lett. **45** (1984) 1229.
- 2) E. Tokumitsu, Y. Kudou, M. Konagai and K. Takahashi: J. Appl. Phys. **55** (1984) 3163.
- 3) K. Kamon, S. Takagishi and H. Mori: J. Cryst. Growth **73** (1985) 73.
- 4) J. A. Lebens, C. S. Tsai, K. J. Vahara and T. F. Kuech: Appl. Phys. Lett. **56** (1990) 2642.
- 5) J-F. Fan and K. Toyoda: Appl. Sur. Sci. **60/61** (1992) 765.
- 6) K. Ozasa, T. Ye and Y. Aoyagi: J. Vac. Sci. & Technol. A **12** (1994) 120.
- 7) K. Nakai and M. Ozeki: J. Cryst. Growth **68** (1984) 200.
- 8) M. Yamada, Y. Ide, K. Tone: Jpn. J. Appl. Phys. **31** (1992) L721.
- 9) K. Watanabe, M. Momose, K. Hara, H. Munekata and H. Kukimoto: J. Cryst. Growth **169** (1996) 223.
- 10) M. Passlack: Appl. Phys. Lett. **66** (1995) 625.
- 11) M. Takeya, Y. Sugimoto, H. Hideya and K. Akita: J. Appl. Phys. **67** (1990) 4297.
- 12) S. H. Jones and K. M. Lau: J. Electrochem. Soc. **134** (1987) 3149.
- 13) S. Adachi: Appl. Phys. Lett. **58** (1985) R1.
- 14) M. Passlack, E. F. Schubert, W. S. Hobson, M. Hong, N. Moriya, S. N. G. Chu, K. Konstadinidis, J. P. Mannaerts, M. L. Schoes and G. J. Zydzik: J. Appl. Phys. **77** (1995) 686.
- 15) H. D. Chen, C. Y. Chang, K. C. Lin, S. H. Chan, M. S. Feng, P. A. Chen, C. C. Wu and F. Y. Juang: J. Appl. Phys. **73** (1993) 7851.
- 16) H. Kawai, K. Kaneko and N. Watanabe: J. Appl. Phys. **56** (1984) 463.